REPUBLIC OF TÜRKİYE

YILDIZ TECHNICAL UNIVERSITY

GRADUATE SCHOOL OF SCIENCE AND ENGINEERING

DETERMINATION OF THE RADIATION DOSE LEVEL TO WHICH THE LUNG AND LIVER ARE EXPOSED IN THE TREATMENT OF LIVER CANCER WITH THE Yttrium-90 RADIOEMBOLIZATION METHOD

Kaan Selçukhan SAKMAK

MASTER OF SCIENCE THESIS

Department of Biomedical Engineering

Biomedical Engineering Program

Supervisor

Assoc. Prof. Dr. Osman GUNAY

July, 2024

REPUBLIC OF TÜRKİYE

YILDIZ TECHNICAL UNIVERSITY

GRADUATE SCHOOL OF SCIENCE AND ENGINEERING

DETERMINATION OF THE RADIATION DOSE LEVEL TO WHICH THE LUNG AND LIVER ARE EXPOSED IN THE TREATMENT OF LIVER CANCER WITH THE Yttrium-90 RADIOEMBOLIZATION METHOD

A thesis submitted by Kaan Selçukhan SAKMAK in partial fulfillment of the requirements for the degree of **MASTER OF SCIENCE** is approved by the committee on 29.07.2024 in Department of Biomedical Engineering, Biomedical Engineering Program.

Assoc. Prof. Dr. Osman GÜNAY
Yıldız Technical University
Supervisor

Approved By the Examining Committee

Assoc. Prof. Dr. Osman GÜNAY, Supervisor
Yildiz Technical University _____

Prof. Dr. İskender AKKURT, Member
Süleyman Demirel University _____

Assoc. Prof. Dr. İsmail CANTÜRK, Member
Yildiz Technical University _____

I hereby declare that I have obtained the required legal permissions during data collection and exploitation procedures, that I have made the in-text citations and cited the references properly, that I haven't falsified and/or fabricated research data and results of the study and that I have abided by the principles of the scientific research and ethics during my Thesis Study under the title of "Determination Of The Radiation Dose Level To Which The Lung And Liver Are Exposed In The Treatment Of Liver Cancer With The Yttrium-90 Radioembolization Method" supervised by my supervisor, Assoc. Prof. Dr. Osman GÜNAY. In the case of a discovery of false statement, I am to acknowledge any legal consequence.

Kaan Selçukhan SAKMAK

Signature

Dedicated to my family

ACKNOWLEDGEMENTS

I would like to thank my thesis advisor, Associate Professor Osman Günay, who guided me with his ideas and opinions throughout my thesis work. The suggestions he gave to shape my thesis and establish it on a scientific basis guided me throughout the study. His interest throughout my thesis writing process and his accessibility at any time played a very important role in the finalization of my thesis.

I would like to express my deepest gratitude to my beloved wife, Bahar Demirhan Sakmak, whose support has been my greatest source of strength throughout this journey. I would like to thank my mother and father, who were always by my side with their constant encouragement, wisdom and guidance throughout the thesis process. I am grateful to Batuhan Sakmak, whose opinion I received on many issues during the thesis process, for his important contributions to making my thesis available. I would also like to thank my friends Erdi Dede and Büşra Öztürk for their unwavering support during my master's degree process. Their support was very important in bringing this thesis to its current form.

Kaan Selçukhan SAKMAK

TABLE OF CONTENTS

LIST OF SYMBOLS

α	Alpha
Bq	Becquerel
β	Beta
γ	Gamma
GBq	GigaBecquerel
Gr	Gray
MeV	Megaelectron Volt
Sv	Sievert
SI	System International
Y	Yttrium
Y-90	Yttrium-90

LIST OF ABBREVIATIONS

AFP	Alphafetoprotein
ALARA	As Low As Reasonably Achievable
BCLC	Barcelona Clinic Liver Cancer
CRC	Colorectal Cancer
CT	Computer Tomography
EPA	U.S Environmental Protection Agency
ET	Extrathoraric
GIST	Gastrointestinal Stromal Tumor
HAI	Hepatic Artery Infusion
HCC	Hepatocellular Carcinoma
ICRP	International Commission on Radiological Protection
IR	Ionizing Radiation
LGA	Left Gastric Artery
LHA	Left Hepatic Artery
MOSFET	Metal Oxide Semiconductor Field Effect Transistor
MRI	Magnetic Resonance Imaging
NIR	Non-ionizing Radiation
NSCLC	Non-small Cell Lung Cancer
OSL	Optically Stimulated Luminescence
PBT	Potency Beam Therapy
PMT	Photomultiplier
PVT	Portal Vein Thrombosis
RHA	Right Hepatic Artery
SBRT	Stereotactic Body Radiotherapy
SCLC	Small Cell Lung Cancer
SMA	Superior Mesenteric Artery
TACE	Transarterial Chemoembolization
TARE	Transarterial Radioembolization
TL	Thermoluminescence
TLD	Thermoluminescence Dosimeter

LIST OF FIGURES

LIST OF TABLES

ABSTRACT

Determination Of The Radiatıon Dose Level To Which The Lung And Liver Are Exposed In The Treatment Of Liver Cancer With The Yttrium-90 Radioembolization Method

Kaan Selçukhan SAKMAK

Department of Biomedical Engineering

Master of Science Thesis

Supervisor: Assoc. Prof. Dr. Osman GUNAY

Liver tumors are examined in two groups, primary and metastatic, and the primary treatment methods are resection. When liver tumors are examined, it is seen that the most common liver tumor is hepatocellular carcinoma. The fact that resection cannot be applied to all patients with liver cancer causes alternative methods to be used in the treatment of the disease. One of these methods, the Y-90 Radioembolization method, is based on the principle of shrinking or destroying the existing tumor by injecting Yttrium-90, which is used as a radionuclide in the treatment of liver tumors and produces β radiation, through the hepatic arteries that largely feed the liver tumor. In this study, a hepatopulmonary shunt model, previously designed in 3D and in which radioembolization treatment, with a hepatopulmonary shunt rate of 10%, can be easily simulated, was used as a phantom. Two tumors, large and small, were simulated in the liver section of the model used and Yttrium-90 was injected into this area. After the radionuclide substance was kept in the relevant tumor cavities for 14 days, radiation dose measurements were made on the lung and liver with the help of thermoluminescence dosimeters. As a result, the highest dose level to which the

lung was exposed was measured between 1.4091 Sv and 1.845 Sv, while the dose to which the liver was exposed was measured as 19.79 Sv to 25.077 Sv. When the half-life of the radionuclide used was evaluated, it showed that the dose levels obtained at the end of the 14th day could be evaluated as the dose levels used in current treatment methods, and although the injected radionuclide did not show a homogeneous distribution, it gave information about the dose level to which the surrounding tissues were exposed.

Keywords: Liver tumor, hepatopulmonary shunt model, Yttrium-90 readioembolization, determination of radiation dose level.

ÖZET

Karaciğer Kanserinin Yttrium-90 Radyoembolizasyon Yöntemi İle Tedavisinde Akciğer Ve Karaciğerin Maruz Kaldiği Radyasyon Doz Düzeyinin Belirlenmesi

Kaan Selçukhan SAKMAK

Biyomedikal Mühendisliği Anabilim Dalı

Yüksek Lisans Tezi

Danışman: Doç. Dr. Osman GUNAY

Karaciğer tümörleri, primer ve metastatik olmak üzere iki grupta incelenmekte ve birincil tedavi yöntemleri rezeksiyon (parça alma) olarak karşımıza çıkmaktadır. Karaciğer tümörleri incelendiğinde ise en sık karşılaşılan karaciğer tümörünün, hepatosellüler karsinoma olduğu görülmektedir. Rezeksiyon işleminin karaciğer kanseri olan tüm hastalarda uygulanamaması, hastalığın tedavisinde alternatif yöntemlere başvurulmasına neden olmaktadır. Bu yöntemlerden biri olan Y-90 Radyoembolizasyon metodu, karaciğer tümörü tedavisinde radyonüklid olarak kullanılan ve β ışıması yapan Yttrium-90'ın karaciğer tümörünü büyük ölçüde besleyen hepatik arterlerden enjekte edilerek, mevcut tümörün küçültülmesi veya yok edilmesi prensibine dayanmaktadır. Bu çalışmada daha önceden 3 boyutlu olarak tasarlanan, hepatopulmoner şant oranı %10 olarak değerlendirilen radyoembolizasyon tedavisinin kolay bir şekilde simüle edilebildiği bir hepatopulmoner şant modeli, fantom olarak kullanılmıştır. Kullanılan modelin karaciğer bölümünde büyük ve küçük olmak üzere iki adet tümör simüle edilmiş ve

bu bölgeye Yttrium-90 enjekte edilmiştir. Radyonüklid madde ilgili tümör boşluklarında 14 gün bekletildikten sonra akciğer ve karaciğer üzerinde termolüminesans dozimetreler yardımı ile radyasyon doz ölçümleri yapılmış, sonuç olarak akciğerin maruz kaldığı doz seviyesinin en yüksek değerleri 1.4091 Sv ile 1.845 Sv arasındayken karaciğerin maruz kaldığı doz 19.79 Sv ile 25.077 Sv olarak ölçülmüştür. Kullanılan radyonüklidin yarılanma ömrü değerlendirildiğinde 14. günün sonunda elde edilen doz seviyelerinin mevcut tedavi yöntemlerinde kullanılan doz seviyelerinin değerlendirilebileceğini göstermiş, enjekte edilen radyonüklidin homojen dağılım göstermemesine rağmen çevre dokuların maruz kaldığı doz seviyesi hakkında bilgiler vermiştir.

Anahtar Kelimeler: Karaciğer Tümörü, Hepatopulmoner Şant Modeli, Yttrium-90, Radyoembolizasyon, Radyasyon Doz Seviyesinin Belirlenmesi.

1
INTRODUCTION

1.1 Introduction

Liver cancer, which is the 6th most common cancer type in the world, is the 4th type of cancer that causes the most deaths [1]. The primary treatment method for liver tumors, which are divided into two groups as primary and metastatic, is resection [2,3]. However, the limited number of patients who can undergo resection for the treatment of liver tumors has made transplantation, ablation, systematic treatments and locoregional treatments alternatives in the treatment of the disease[3]. The most common primary liver tumor is Hepatocellular carcinoma (HCC), with a rate varying between 75% and 85% [4]. Radioembolization treatment with Yttrium-90, one of the methods used in the treatment of HCC, will form the basis of this study. Yttrium-90 radioembolization treatment is performed by injecting Yttrium-90 radionuclide, which emits beta radiation, into the tumor tissue or tissues in the liver through the hepatic artery. Yttrium-90 microspheres injected into the tumor area via the hepatic arteries, which constitute approximately 70-80% of the vessels feeding HCC, offer a more localized treatment option by adhering directly to the tumor part. The low tissue penetration of the beta ray emitted by Yttrium-90 microspheres causes the surrounding healthy tissues to be less affected by radiation[5]. Figure 1 schematically shows how yttrium-90 radioembolization treatment is performed[6]. Transarterial treatment of Yttrium-90 is visualized in Figure 2[6].

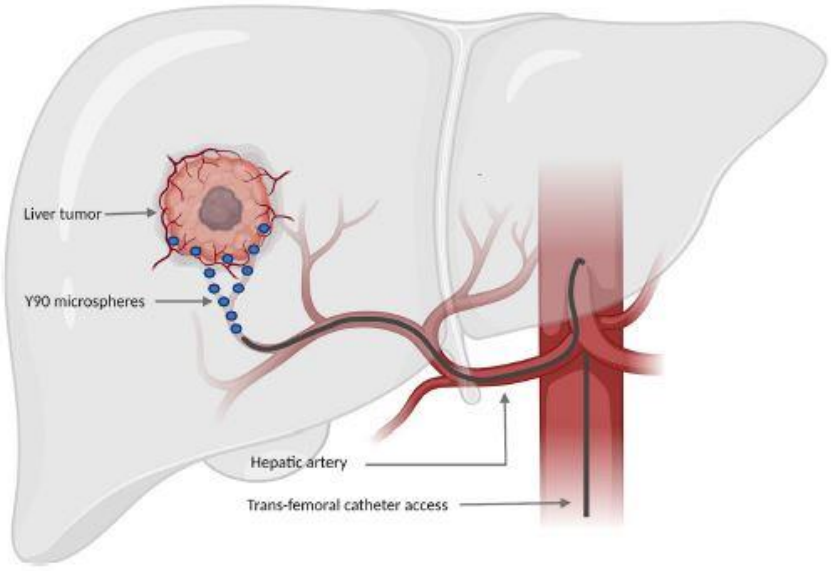

Figure 1 Schematic of Yttrium-90 radioemolization treatment[6]

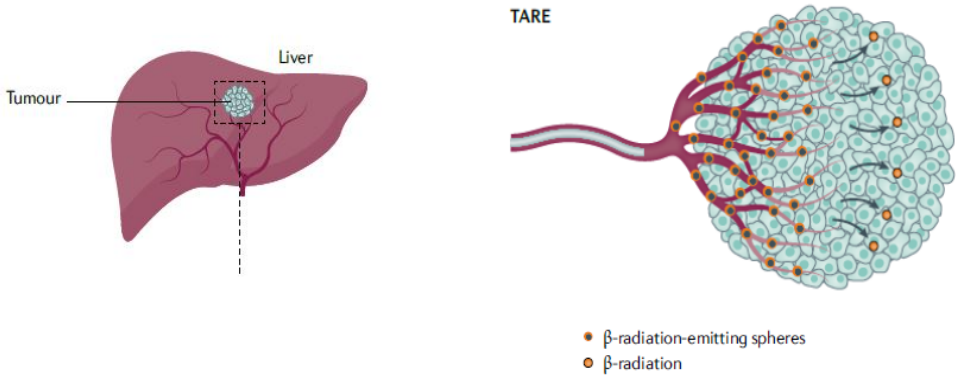

Figure 2 Yttrium-90 microspheres reach the tumor tissue with the help of hepatic arteries and beta radiation penetrates the tumor tissue[6].

In addition to the positive effects of radioembolization treatment, there are also factors that need to be taken into consideration. Considering the general principles of treatment, 90Y-microspheres are located in the inner part of the hepatic arteries that feed the tumor. However, 90Y-microspheres may establish a direct vascular access to the lungs via arteriovenous vascular shunts, resulting in lung exposure to radiation. In order to prevent this situation, the hepatopulmonary shunt rate must be calculated correctly and the dose level to be applied in treatment must be determined by taking this rate into consideration. A hepatopulmonary shunt model prepared by Yeyin et al was used in this study. The shunt model was created by fixing both lobes of the liver and lung in a plexiglass box. As a result of the study conducted by Yeyin et al., the hepatopulmonary shunt rate was measured as 10.2%[7].

Although the use of radiotherapy in cancer treatment works to shrink or destroy the targeted cancer cell, it may expose healthy tissues to the adverse effects of radiation. Therefore, in evaluating the effectiveness of current treatment methods, it is important to determine the dose levels to which healthy tissues are exposed in current treatment methods. In this study, liver tumor treatment was simulated with a 3D hepatopulmonary shunt model. Two tumor cavities, one large and one small, were created in the existing liver model, and Yttrium-90 radionuclides were injected into these cavities, as in Yttrium-90 radioembolization treatment. The phantom showing large and small tumors in the liver is as seen in Figure 3. The 10% value obtained in the study by Yeyin et al. was considered as the hepatopulmonary shunt rate and a dose of 2 GBq was applied to the tumor area for treatment. Taking into account parameters such as the half-life of the radionuclide used, the radionuclide was left in the liver phantom for 14 days, and the dose levels exposed to the liver, lungs and the corners of the plexiglass and the surrounding organs modeled were measured with TL dosimeters, and the effectiveness of the treatment and how healthy tissues would be affected by the dose levels they were exposed to were tried to be determined. While conducting the study, it was taken into account that the lung is one of the most radiosensitive organs. An attempt was made to evaluate whether there was a dose level that could cause discomfort such as pneumonitis, which usually occurs 1 to 3 months after exposure to radiation. In addition, evaluations were made about the dose levels to which healthy and tumor

areas of the liver were exposed. It is considered that the data obtained as a result of the study will constitute valuable data for future studies and may give us ideas on issues such as radiation protection and safe dose use in radiotherapy.

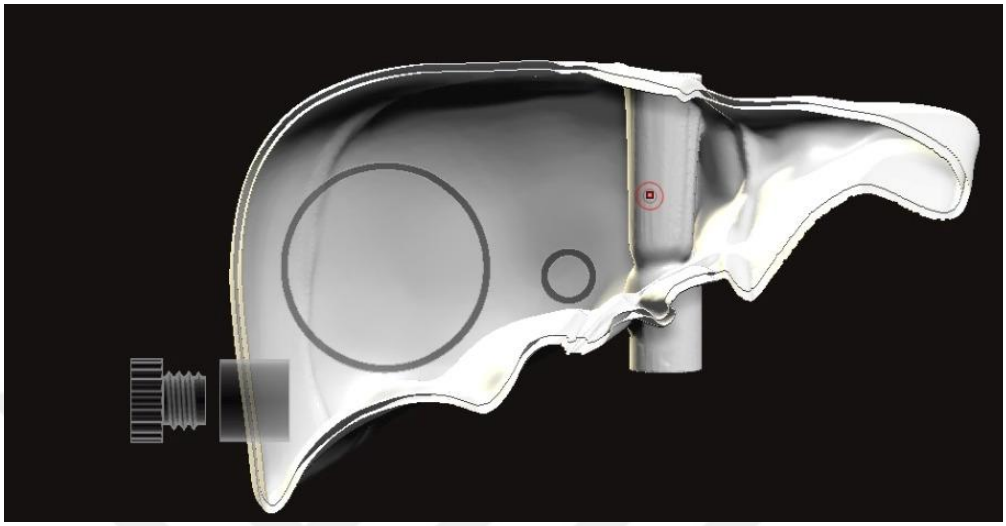

Figure 3 The internal structure of the liver phantom and the appearance of tumors in the internal structure of the phantom[7].

2
GENERAL INFORMATION

2.1 Radiation

Radiation, which is examined in two groups as particle radiation and electromagnetic radiation, can be defined as the spread of energy through particles or electromagnetic waves in space or in a concrete environment[8]. The discovery of X-rays by Wilhelm Roentgen in 1895 is considered one of the turning points in the history of radiation and medicine[9]. When radiation is examined from historical perspective, after the discovery of the X-ray, Henri Becquerel's discovery of radioactivity in 1896, and joseph John Thomson's free electron studies in 1897 are considered important discoveries. These studies were followed by the discovery of Polonium and Radium by Marie and Pierre Currie, which was also a very important discovery for the history of radiation. The importance of this discovery is explained by the fact that the substances are radioactive. The radioactive properties of these elements allowed them to pass through solid materials and emit invisible rays that conduct electricity[10].

2.1.1 Classification and Properties of Radiation

The sources of radiation, defined as the spread or transfer of energy in the form of electromagnetic waves or particles, are divided into natural and artificial[11]. Another classification criterion of radiation is basically its ability to release the electrons of an atom and cause the atom to ionize. Non-ionizing radiation (NIR) is a type of radiation that, although it excites the atom, does not have enough energy to remove electrons. Wave types in the electromagnetic spectrum, referred to as radio waves, microwaves, infrared rays and visible light, define NIR types[12]. Ionizing radiation (IR) is defined as the flow of energy in the form of electromagnetic waves or subatomic particles that cause the ionization of an atom, which can release its electrons[13]. Examples of ionizing radiation emitted as electromagnetic waves are X-rays and gamma rays. The types of ionizing radiation emitted as subatomic particles are called alpha, beta and neutron. IR is produced through the spontaneous decay of radioactive elements. In this process, radioactive elements break down into many times smaller atoms. Many radioactive

intermediaries play a role in this decay process, and this process is repeated until the elements become stable. Parameters such as speed and radiation type that will be encountered in this process are shaped according to the characteristics of the radioactive elements. Another way of producing IR is by causing charged particles to move quickly and colliding with a substance. X-rays used in imaging devices are also produced this way[14]. Ionizing and non-ionizing radiation types are shown in Table 1[12].

Table 1 Ionizing and non-ionizing radiation and its types are shown.

Ionizing Radiation		**Non-ionizing Radiation**
Alpha	X-ray	Radiowave
Beta	Gamma ray	Microwave
Neutron		Infrared
		Visible light

2.1.1.1 Alpha Particles

One of the famous studies on alpha particles was conducted by Earnest Rutherford in 1917 and allowed the understanding of the structure of the atom[9]. Alpha particles consist of two neutrons and can be considered atomically large. Particles with high ionizing properties are very energetic, but their weight and size mean that they lose their energy over short distances. Therefore, they can be stopped by paper or human skin. However, it is of interest in targeted therapy due to the same properties. The most important reason for this interest is that it provides specifity to target a selected cell population with minimal effect on-targeted cells[15].

The fact that alpha radiation cannot penetrate human skin due to the above-mentioned properties means that it can almost not harm humans through extracorporeal interaction. In addition, if inhaled or swallowed, they can cause a high level of focused ionization. They give all their energy to the few cells they focus on. Thus, they can cause serious damage at the cellular and genetic level in

the region where they transfer their energy[9]. Alpha decay is shown in Figure 4[16].

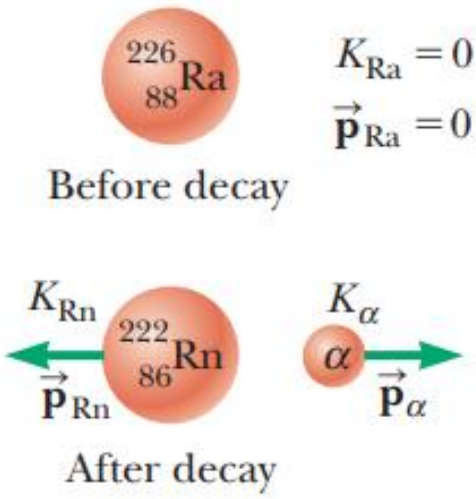

Figure 4 Alpha decay of Radium is shown.

2.1.1.2 Beta Particles

Beta particles (β) are a type of radiation that occurs when the ratio of neutrons to protons in the atomic nucleus is high. While the high amount of neutrons turns into a proton or electron, the electrons are thrown out with high energy. The proton remains in the nucleus[9]. The way Beta decay of the carbon element occurs is shown in Figure 5[18]. Compared to alpha particles, the penetration properties of beta particles are much stronger. However, to effectively reduce the effects of beta radiation, it is sufficient to use protection methods such as thin plastic and glass materials[17]. The 2 MeV beta particle is known to have a range of 1 cm in water. This feature makes it extremely important for treatments where tissue penetration is not desired. The uses of beta radiation are similar to x-rays and other types of radiation. When the effects of irradiation are examined, it is seen that it is destructive. There must be a distinctive sensitivity between healthy tissue cells adjacent to the pathological cells that beta particles, a type of radiation also used in tumor treatment, will destroy. In this study, Yttrium-90, which emits pure beta radiation, was used as a radionuclide. The activity of beta radiation, which cannot normally be visualized with CT, can be visualized on CT with the Bremsstrahlung method.

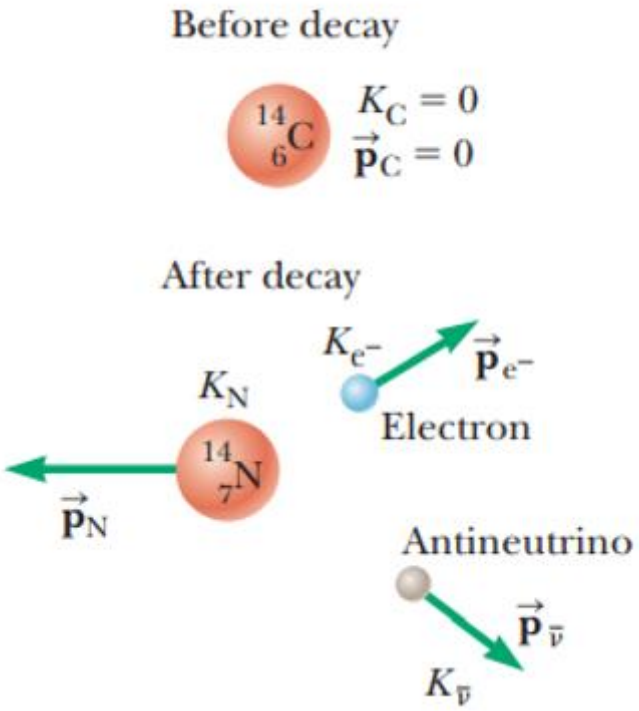

Figure 5 How Beta decay of the element carbon occurs.

2.1.1.2.1 Bremsstrahlung Radiation

Bremsstrahlung can also be called radiation slowing down. It occurs when a charged particle slows down due to the effect of the nuclear field and loses some or all of its energy while passing through matter[19].

2.1.1.3 Gamma Radiation

Gamma radiation, which is known to have no mass or charge, is transmitted from the radioactive nuclide as photons, not as particles like alpha and beta radiation. This type of radiation, which has no mass, has a strong penetration ability. Thanks to these properties, they can easily pass through living organisms. Gamma radiation is used for treatment purposes in various areas of Dermatology. One of the most important radionuclides that decays in the form of gamma radiation is Technetium-99. The fact that gamma rays have the shortest wavelength and highest amount of energy causes them to be used in studies in many different fields. The gamma decay of the boron element is shown in Figure 6[20].

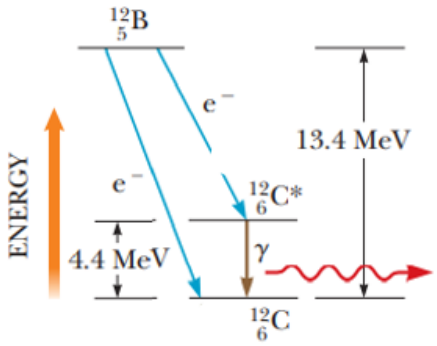

Figure 6 Formation of Gamma decay of the boron element

2.1.1.4 Neutron Particles

The uncharged particle found in the atomic nucleus is called a neutron. Neutron particles, which are uncharged, do not interact with orbiting electrons, and this feature allows them to easily pass through the target nucleus. These particles with high penetration power are obtained by nuclear reactions in the atomic nucleus[12]. Considering these properties, the interactions of neutrons with matter were examined. It has seen potential to play a critical role in nuclear energy and radiation protection applications[21].

2.1.1.5 X-rays

X-rays, by Wilhelm Roentgen during his studies on cathode light in a glass tube, have been one of the most used types of electromagnetic radiation since the day they were discovered. X-rays basically arise as a result of moving electrons interacting with matter[22]. Unlike gamma rays, another type of electromagnetic radiation, X-rays emit from outside of the atomic nucleus, not from inside it. The penetration ability of X-rays, which can be both naturally occurring and artificially produced by machines, is low due to their low energy levels. In addition to being used in imaging of bones and soft tissues in the medical field, they are also actively used in safety controls and industrial quality and process controls. This wide range of uses makes them one of the most exposed types of ionizing radiation[9].

2.1.2 Radiation Dose Units

The increase in the use of radiation during processes such as diagnosis and treatment in healthcare practices and the clear definition of its negative effects over the years have made it necessary to measure the radiation to which both patients and healthcare professionals are exposed[12]. Various dose measurement methods and

units are used to accurately define and classify the radiation to be measured. In order to makte the units used traceable, the International Comission on Radiological Protection (ICRP) has carried out studies and determined the units to be used for quantities such as activity dose, absorption dose and equivalent dose. In 1997, it was adapted with System International (SI) units and the units used today were adopted[23].

2.1.2.1 Absorbed Dose

The dose used to define the amount of radiation exposure of the human body is called absorbed dose. Gray (Gy), used as the measurement unit, shows the amount of absorption of radiation by one kilogram of matter. In absorbed dose measurement, instead of dealing directly with the radiation itself (for example, its type and properties), the state of the substance exposed to radiation is evaluated[24]. Since Gray is a very large quantity in absorbed dose measurements, units such as nanogray (nGy), microgray (μGy) and miligray (mGy) are generally used[25].

2.1.2.2 Equivalent Dose

Equivalent dose indicates the amount of radiation absorbed by tissues or organs and has harmful biological effects. The unit of equivalent dose is expressed in Sievert (Sv), which shows the effects of exposed radiation on living beings. As it is known, each type of radiation has different properties, which makes their biological effects on tissues and organs different from each other. Therefore, the biological effects of a certain amount of radiation applied to a tissue and organ may vary[25]. To measure the equivalent dose, a mathematical formula based on multiplying the absorbed dose by the radiation weight factor is used[24]. Since the radiation weight factor specified in the formula is unique for each type of radiation, it clearly shows the differences between radiation types even if the energy accumulation levels are the same[25].

$$H_T = W_R \,.\, D_{T,R}$$

H_T = Equivalent dose

W_R= Radiation weighting factor

$D_{T,R}$ = It is the dose absorbed by the tissue or organ according to the type of radiation[27].

Table 2 Recommended radiation weighting factors from International Commission On Radiological Protection (ICRP)

Radiation Type	**Radiation Weighting Factor**
Photons (X-ray and gamma ray)	1
Electrons	1
Alpha Particles	20
Protons	1

2.1.2.3 Effective Dose

Effective dose is a term used to express the risk that the current dose received by tissues and organs carries for the whole body after exposure to a radiation source. As with the equivalent dose, the unit of measurement of the effective dose is the Sievert. It is also generally defined as the weighted average of the dose absorbed by various organs and tissues. The weight factor, one of the most important parameters used to calculate the effective dose, indicates the radiation damage caused by whole body irradiation for particular organ or tissues[26]. As a result of studies carried out, the changes in the weight factor according to organs are shown in Table 3 below. As can be seen from the table, the sum of the weight factors of the organs and parts within the body is calculated as 1. Based on this result, it is seen that the dose value that will be effective for the whole body will be reached by adding up the weighted equivalent doses. The effective dose calculation formula is expressed as follows [27].

$$E = \sum_T W_T . H_T$$

E = Effective dose of the whole body

W_T *= Tissue weighting factor of the tissue (T)*

H_T *= Equivalent dose absorption from tissue (T)*[27].

Table 3 Weighting factors according to tissues. Remainder tissue expression shows the total weight of tissues such as adrenals, extrathoraric (ET) region, gall bladder, heart, kidneys, lymphatic nodes, muscle, oral mucosa, pancreas, prostate, small intestine, spleen, thymus, uterus/cervix[27].

Organ	**Tissue Weighting Factor**
Gonads	0.08
Bone marrow	0.12
Colon	0.12
Lung	0.12
Stomach	0.12
Breast	0.12
Bladder	0.04
Liver	0.04
Oesophagus	0.04
Thyroid	0.04
Skin	0.01
Bone (surface)	0.01
Salivary glands	0.01
Brain	0.01
Remainder	0.12
TOTAL	**1**

2.1.3 Radiation Dose Measurement Methods

Radiation dosimeters are systems used to directly or indirectly measure the amount of exposure to ionizing radiation, the absorbed and equivalent dose. While the dosimeter measures the amount of radiation, the reader of the dosimeter enables the measured amount to be displayed. A system to be used as a radiation dosimeter is expected to be able to detect the characteristic features of the quantity to be measured, such as accuracy, precision, dose, dose rate, energy response, direction dependence and spatial resolution[28]. In addition to this information, it is not expected that every dosimeter will display all these features. For this reason, the types of dosimeters to be used vary depending on the type of radiation to be measured and the environment in which the measurement will be made. The types and features of radiation dosimeters will be discussed in the following section.

2.1.3.1 Ionization Chamber Dosimetry Systems

One of the dose measurement methods used in radiotherapy and diagnostic radiology is ionization chambers. In these systems, the dose is determined under reference irradiation conditions. The dose determination process is also called beam calibration. Some features should be common to ionization chambers, which can have various shapes and sizes depending on the type of radiation to be used and the environment in which the measurement will be made[28].

2.1.3.2 Film Dosimeters

One of the dosimeter types used in radiation measurment is film dosimeters. This type of dosimeters are examined in two groups: radiographic and radiochromic. The basis of film dosimetry is based on the use of radiographic x-ray film, which has an important place in diagnostic radiology, radiotherapy and radiation protection, as a radiation detector and relative dosimeter[28]. Radiochromic film dosimeters have all the features of classical radiographic dosimeters and can measure radiation dose without having a wet processor. Another important feature of radiochromic film dosimeters is that they are a dose measurement method can be used in all radiation fields, regardless of beam quality, in a wide energy range. Compared to radiographic film dosimeters, their senstivity to visible light is much lower[29]. The structures of radiographic and radiochromic film dosimeters are shown in Figures 7 and 8[30].

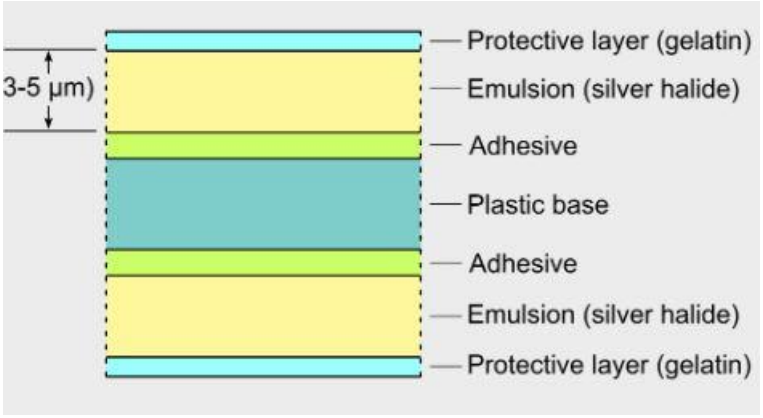

Figure 7 Structure of radiographic film dosimeter

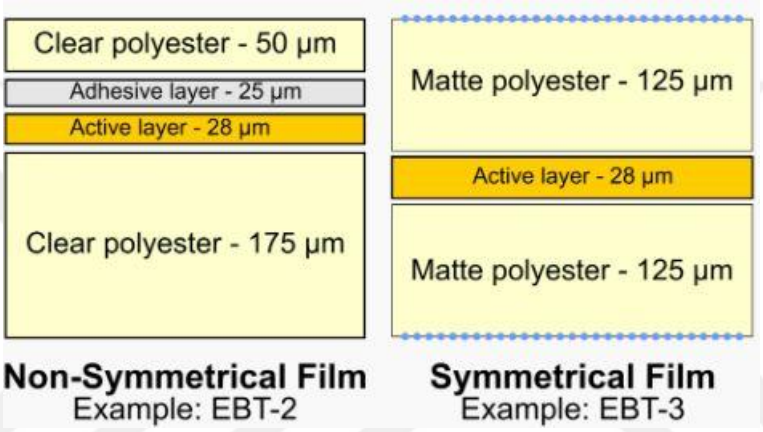

Figure 8 Structure of radiochromic film dosimeter

2.1.3.3 Luminescence Dosimeters

The phenomenon of ultraviolet, infrared and visible light emission that occurs as a result of the absorption of radiation by a material and the retention of a part of absorbed radiation energy in a metastable manner is called luminescence. There are two type luminescence called Fluorescence and Phosphorescence. The feature that distinguishes these luminescent types from each other is the time delay that occurs between stimulation and emission. Additionally, it is known that the phosphorescence process can be accelerated by light or heat stimuli. If the stimulating substance is light, the resulting luminescence phenomenon is called optically stimulated luminescence (OSL). The phenomenon that occurs when the stimulating substance is heat is called thermoluminescence (TL) and radiation measurement is carried out with the help of thermoluminescence dosimeter (TLD) [28].

2.1.3.4 Thermoluminescence Dosimeters (TLD)

The type of dosimeter used in this study is TLD. The most important feature of radiation dosimeters based on the TL phenomenon is that the amount of light emitted and the absorbed dose rate are in proportion. The mentioned ratio allows sensitive and accurate measurement of ionizing radiation. This has made TLDs one of the most used dosimeter types in medicine. The main features sought for the use of thermoluminescence dosimeters in medical fields can be defined as accuracy, senstivity, batch homogenity ,precision and repeatability. Altough TL can be observed on many materials, very few of these materials can meet the requirements of TLD. Table 4 shows the features required for TLDs to be used as medical dosimeters. [30].

Table 4 Requirements of TLDs using for medical dosimetry[30].

Task	**Dose range (mSv)**	**Uncertainty SD (%)**	**Tissue Equivalent**
Whole Dosimetry	0.01-0.5	-30, +50	Important
Radiotherapy	0.1-100	±3.5	Very Important
Diagnostic Radiology	0.001-10	±3.5	Important

The dose amount measured by a TLD dosimeter with the above-mentioned features is calculated by the TLD reader, another part of the dosimeter system. A diagram showing the working principle of a TLD reader is shown in Figure 9.

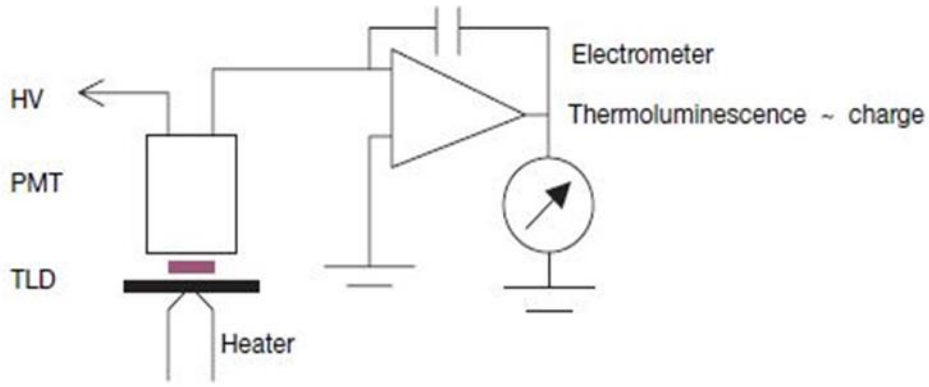

Figure 9 Basic structure of TLD reader [28]

TLD, exposed to the temperature of the type of radiation to be measured produces TL light emission. Thanks to the Photomultiplier Tube (PMT), the detected light emission is converted into an electrical signal. An electrometer is used to convert this electrical signal into a meaningful current or charge value[28].

2.1.3.5 Semiconductor Dosimetry

The use of semiconductor materials, which began to be used as detectors in the 1950s, as radiation dosimeters has increased considerably, and due to their strong properties, these dosimeters produced from semiconductor materials have begun to play critical role in radiation measurement. When the powerful features of these dosimeters are examined, their small size, instantaneous electrical response ability, and stability of sensitivity to ionizing radiation come to the fore. These dosimeters, which are frequently used in radiotherapy, especially in in vivo treatments, due to their small size and fast electrical processing capabilities, are divided- into three groups: diodes, metal-oxide-semiconductor field-effect transistors (MOSFETs) and silicon-dioxide (SiO2)[31].

2.1.4 Radiation Protection Methods and Their Importance

In contemporary medical applications ionizing radiation can seen as an inevitable way to diagnose and treat various medical conditions. Therefore, radiation safety is critical for patients, doctors, and medical personnel in various departments, such as radiology, interventional cardiology, and surgery. Radiation exposure from fluoroscopic procedures poses the highest risk for medical staff due to its significant

radiation doses [32]. Radiation protection methods are important to reduce the risk factors by minimizing the damaging consequences of ionizing radiation [33]. The effects of radiation exposure can be categorized under two dimensions stochastic effects, and deterministic effects [34]. Stochastic effects can be conceptualized as an outcome that might happen with some likelihood, but there is no specific point at which it starts to happen. Therefore, it is hard to diagnose stochastic effects immediately after the radiation exposure. These effects might be revealed after many years. On the other hand, the International Commission on Radiological Protection (ICRP) -118 conceptualized the deterministic effects as "Tissue Reactions" because it is obvious that these effects are not present at the time of irradiation. Tissue reactions refer to injuries occurring in groups of cells where there is a threshold dose, beyond which the severity of the damage intensifies as the dose continues to rise.

There are different approaches in terms of radiation protection methods. According to Frane & Bitterman (2020), it is possible to mention three fundamental protection principles that should be taken into consideration; justification, optimization, and dose limitation [32]. Besides these principles U.S Environmental Protection Agency (EPA) suggests different techniques that are proven to be helpful with radiation protection. EPA highlights that an efficient radiation protection program should include: Qualified Staff, As Low As Reasonably Achievable principle, a dosimetry program, radiological controls, surveys and monitoring, preset emergency procedures, worker training, record keeping, and international audit procedures. At this point, it is crucial to handle the As Low As Reasonably Achievable (ALARA) principle, which includes several methods for a successful radiation protection procedure[35]. The ALARA principle suggests three techniques, which are time, distance, and shielding to prevent medical workers from radiation exposure [36]. While "Time" stands for minimizing the amount of time that is spent in the areas that are polluted with radiation, "Distance" stands for maximizing the distance from the source of the radiation. Also, it is highly recommended to use proper shielding between the source of the radiation and the workers. The type of shielding can be determined by the type of and activity of the radiation source. Interlock systems, which automatically determine the amount of radiation exposed and shut down the entire system, can also be used as protective

factor [35]. Implementing the warning systems and providing the staff with protective equipment is also a significant way to prevent radiation exposure.

2.1.5 Application of Radiation in Medicine

The application of radiation in medical applications has a long history. The first medical applications, which use ionizing radiation date back to the discovery of X-rays and radioactivity in the late 19th century [37]. The first attempts to use radiation in the context of medical therapies included uranium extracts by Standard Company Medical in 1910 [38]. Physicians used radiation exposure in the process of tumor size, slowing down cancer progression, and eliminating cancer metastasis. Because cancer cells are targeted as foreign pathogens by the immune system of the patients, radiation was used to trigger the immune system of the patients [37]. Beside these, radiation was used in different treatment procedures for inflammatory diseases such as asthma, immune system disorders, and arthritis[39]. Additionally, Calabrese et al. (2015) revealed that there was no reported increase in cancer among these patients [40]. Sakamato (1990) also revealed that low doses of total- or half-body radiation (TBI/HBI) can stimulate immunity. Additionally, Sakamoto found that the killing of tumor cells can be enhanced by administering a high dose of radiation locally to the tumor, 12 hours after delivering 0.1 Gy of TBI. Furthermore, he demonstrated that distant metastases can be suppressed by TBI treatments of 0.1 or 0.15 Gy [41].

Calabrese et al, (2019) identified several studies investigating the appropriate dosing that should be used in radiotherapy. The results came from the studies that were implemented from 1910 to 1950 (Table 5). According to the results, the proper dosing should be considered while radiotherapy practices found to be between 30 to 100 rads. Calabrese et al, (2019) also conclude that these studies indicated that low doses of radiation, similar to certain chemical agents, could mediate anti-inflammatory effects by influencing macrophage polarization towards an anti-inflammatory phenotype [42].

Table 5 Diseases/Conditions that are treated with radiotherapy intervention[42].

	Number of Cases	**Successful Treatment Rates(%)**	**Studies (N)**	**References (Calabrese et al., 2019)**
Arthisis	>5000	~ 85	Cumulative Experience	Kahlmeter and Kuhnsand, Morrison
Bronchial Asthma	~4000	75-80	57	Calabrese et al.
Carbuncles	187	60-90	5	Calabrese
Cervical adenitis	893	75-90	11	Calabrese and Dhawan
Deafness	15000	>95% Performed before age 15	Cumulative Experience	Calabrese and Baylor
Furuncles	420	75-95	5	Calabrese
Gas gangrene	365	Mortality rate decreased from 40% to 10%	Cumulative Experience	Calabrese and Dhawan
Otitis media/mastoides	564	~90	16	Calabrese and Dhawan
Pertussis	~2400	~80	22	Calabrese et al.

Table 5 Diseases/Conditions that are treated with radiotherapy intervention[42]. (continued)

Pneumonia	864	80-85	18	Calabrese and Dhawan
Sinus infection	4492	75-90	16	Calabrese and Dhawan
Tendonitis/bursitis	3333	70-90	31	Calabrese and Dhawan

2.2 Anatomy of Liver

The liver, the largest organ of the human body, weighs an average of 1200-1400 grams in women and 1400-1600 grams in men[43]. Liver anatomy is examined in two groups: morphological and functional. While the morphological classification deals with the external appearance of the liver, functional classification examines the structures of the liver and the functional properties of the bile ducts [44]. The segmental anatomy of the liver plays an important role in the localization and treatment of focal lesions. When the studies on segmental anatomy are examined, the studies of Goldsmith and Woodburne, who studied hepatic segmental anatomy and created a system, based on the distribution of hepatic veins, did not allow access to the necessary information for subsegmental hepatic resection planning. Laetr, modification of this model by Couinaud and Bismuth, respectively, by evaluating the portal and hepatic veins together, provided access to the necessary information surgically [43].

In the study modified by Couinaud, the liver was divided into 8 different segments that worked independently of each other. In this classification, the middle hepatic vein divides the liver into right and left lobes, and the right lobe into anterior and posterior segments. The left hepatic vein divides the left lobe into medial and lateral segments. The portal vein separates the upper and lower segment of the liver. Bismuth modified this model in his study[44]. The classifications made by Couinaud, Bismuth and Goldsmith/ Woodburne are shown in Table 6.

Table 6 Naming the anatomical segments of the liver, comparing existing studies on this subject [43].

Anatomical subsegments	**Couinaud**	**Bismuth**	**Goldsmith/Woodburne**
Caudate lobe	I	I	Caudate lobe
Left lobe lateral superior segment	II	II	Left lobe lateral segment
Left lobe lateral inferior segment	III	III	
Left lobe medial segment	IV	IVa, IVb	Left lobe medial segment
Right lobe anterior inferior segment	V	V	Right lobe anterior segment
Right lobe anterior superior segment	VIII	VIII	
Right lobe posterior inferior segment	VI	VI	Right lobe posterior segment
Right lobe posterior superior segment	VII	VII	

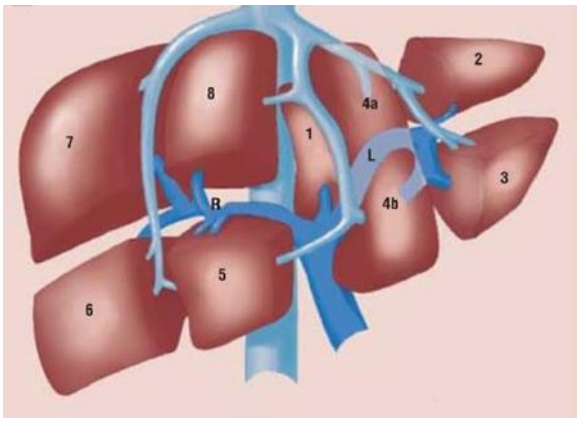

Figure 10 Couinaud liver segments. R shows right portal vein; L shows left portal vein. Unlabeled braches indicates hepatic vein anatomy[45].

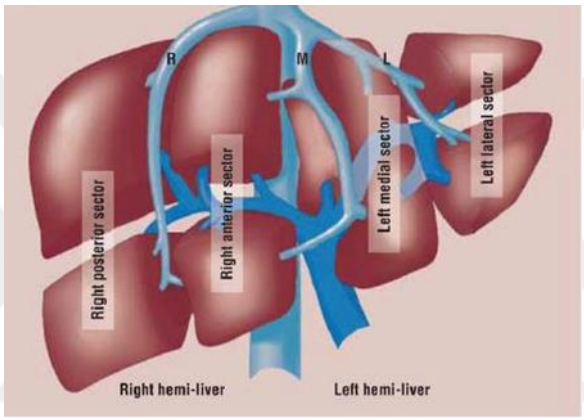

Figure 11 It shows hepatic veins, R indicates right, M indicates middle, and L shows left[45].

2.2.1 Liver Vascular Anatomy

Knowing the vascular anatomy of the liver is extremely important for the evaluation and planning of the technique of hepatic arterial treatments, which play an important role in the treatment of liver tumors. Transport of blood to the liver occurs through the portal vein and hepatic arteries[44]. The amount of blood carried by the hepatic artery to the liver id approximately 25-30%[43]. The remaining part is carried to the liver by the portal vein. In addition, these two sources meet the liver's oxygen needs[44]. It is known that it has an important role in the treatment of liver tumors, and many variations can be seen when the anatomy of the hepatic arteries is examined. Knowing these variations is critical to predict and maintain treatment processes in a healthy way. The first grouping process on this subject was carried

out by Michels in 1955. In his study, Michels named the standard hepatic arterial anatomy, which has a slice of approximately 55%, as type 1, and classified the variations between type 2 and type 10[43].

Table 7 Classification of hepatic artery variations made by Michels in 1955[43]. LHA shows Left Hepatic Artery, RHA shows Right Hepatic Artery, LGA shows Left Gastric Artery, SMA shows Superior Mesenteric Artery.

Types	**Frequency (%)**	**Description**
I	55	Standart
II	10	Replaced LHA
III	11	Replaced RHA
IV	1	Replaced LHA and RHA
V	8	Accessory LHA arising from the LGA
VI	7	Accessory RHA arising from the SMA
VII	1	Accessory LHA and RHA
VIII	2	Accessory RHA and replaced LHA or Accessory LHA
IX	4.5	Common Hepatic Arter originates from the SMA
X	0.5	Common Hepatic Arter originates from the LGA

2.2.2 Liver Tumors

Liver tumors can occur as malignant or benign. Another classification of liver tumors is based on their origin in the liver and spread from extrahepatic primary tumors. While tumors originating from the liver are called primary liver cancer, tumors that spread from primary tumors are called metastatic liver cancer. When malignant liver tumors are examined, Hepatocellular carcinoma (HCC) and cholangiocarcinoma appear as two huge tumors. Extrahepatic primary tumors are considered as colorectal, lung and pancreatic cancers, and these cancer types cause liver metastasis[46].

2.2.2.1 Primary Liver Tumors

The most common of the primary liver tumors is HCC. Studies show that HCC is the third cancer type that most causes death in the world. Generally, HCC appears to be the sixth most common type of cancer in the world[47]. The main causes of this deadly type of cancer are Hepatitis B and C, obesity chronic liver diseases and cirrhosis[48]. Abnormalities encountered on liver imaging of a patient known to have one of the diseases mentioned above usually indicate HCC. Imaging is performed with ultrasound devices as well as computed tomography (CT) and magnetic resonance imaging (MRI) devices. Additionally, examining suspicious tissue by taking a biopsy is a frequently used method [49]. It is the amount of alphafetoprotein (AFP) that has an important place in diagnosing. Studies show that AFP levels increase in 60-70% of patients diagnosed with HCC. In suspicious cases where there is no significant change in AFP level, imaging of the liver is performed using more complex imaging methods such as CT and MRI[43].

When HCC treatment is evaluated, it is seen that the process of dividing the disease into stages is very important. There are various studies in this context. These studies examine and recommend creating treatment plans according to the characteristics of the tumor, history of liver disease, and current status of the disease[44]. Although treatment staging studies are on a similar basis, they are not universally accepted. Barcelona-Clinic-Liver-Cancer (BCLC) staging system, one of these studies, was created and started to be used by examining various disease stages and treatment methods[49]. The diagram showing the general flow of the BCLC staging system is shown in Figure 12.

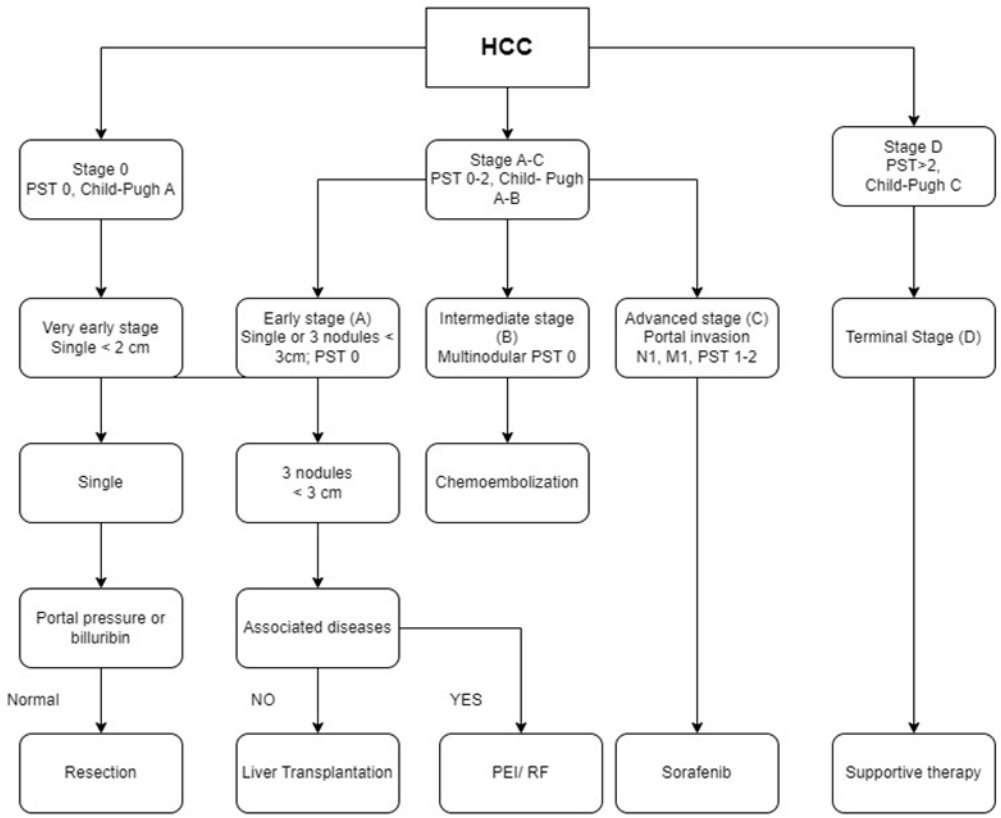

Figure 12 BCLC stages and treatment processes in liver cancer [43].

2.2.2.2 Metastatic Liver Tumors

Cancer that starts in a specific organ or tissue and spreads to a region far from the organ or tissue where it started are named metastatic cancer. When naming metastatic cancers, the name of the primary cancer that is the source of the cancer is taken into account. Primary cancer that spreads to a different organ is not named after the organ to which it has spread. Treatment is applied as the 4^{th} stage of primary cancer[50]. When metastatic cancers were examined in terms of the liver, it was seen that the cancer that most metastasized to the liver was colorectal cancer (CRC). When other types of cancer that metastasize to the liver are considered, we encounter pancreatic cancer, breast cancer, melanoma and lung cancer[51]. The liver is one of the organs most frequently metastasized in the body [44]. The reason for this situation is thought to be that the liver has an extremely rich blood supply. In addition, CRC, pancreatic cancer and neuroendocrine tumors, which are found in the gastrointestinal tract and cause liver metastasis, and gastrointestinal stromal tumors (GIST), which are less common than these are. Exposure to venous blood returning using the portal vein circulation within this system is one of the reasons

for liver metastasis. Beside these, the metastasis rates of the cancer types that most commonly metastasize to the liver as the primary tumor are shown in Table 8[51].

Table 8 Percentage of common primary cancers metastasizing to the liver.

Primary Cancer	**Percentage (%)**
Small cell lung cancer (SCLC)	17
Non-small cell lung cancer (NSCLC)	4
Cutaneous melanoma	10-20
Breast cancer	6-38
Colorectal cancer	30-50
Pancreatic cancer	30-40
Gastric cancer	5-40
Neuroendocrine tumor	20-46

- **Liver Metastasis Treatment Methods and Management of the Treatment Process**

In the treatment of liver metastases, the treatment process is carried out according to a program prepared by a multidisciplinary team that will increase the efficiency of this process. This multidisciplinary team includes surgeons, radiologists, oncologists and pathologists[51]. Valid treatment methods that can be applied in the treatment of liver metastases are listed in Table 9.

Table 9 Treatment methods can be applied in the treatment of liver metastases.

Treatment Methods	**Purpose of Treatment**
Surgery	If the metastasis is resectable, resection is the main treatment procedure planned to be used[51]. Especially in the treatment of CRC, resection is the best option[52].
Transplantation	Liver transplantation is not a common practice in the treatment of liver metastases[51].
Ablative Therapies	Although resection is the best treatment option for metastases, only 20-30% of patients are suitable for this procedure. For this reason, alternative methods are also used in the treatment of metastasis. Ablation treatment is applied with radiofrequency, microwave and cryotherapy methods. It is one of the treatment methods used with low complication rates [53].
Systemic Therapy	It is a treatment method performed with the use of molecular targeted agents. It has been developing rapidly since the early 2000s[51].
Locoregional Therapy	Locoregional treatment methods include methods such as hepatic artery infusion (HAI), transarterial chemoembolization (TACE), potency beam therapy (PBT) and stereotactic body radiotherapy (SBRT), which aim to reduce the complication rate of other tissues and organs by localizing the treatment[51]. The transarterial radio-embolization method, which is the treatment method that forms the basis of the study, will be discussed in more detail.

- **Transarterial Embolization**

The place of transarterial radioembolization (TARE) with Yttrium-90 in the treatment of liver tumors is increasing day by day due to the positive effects it provides[54]. Studies on the TARE method, which was developed as a locoregional treatment method in the treatment of HCC, have been continuing since the 1960s. The fact that it has fewer complications compared to existing locoregional treatment methods and that this situation is supported by studies has made TARE one of the most used treatment methods in the treatment of liver tumors[55].

The Y90 radioembolization method, whose effectiveness was investigated in the treatment of patients diagnosed with portal vein thrombosis (PVT), which is estimated to occur in one in every 3 patients with HCC, was determined to be highly effective in this treatment by Salem et al. in 2004[56].

In radiotherapy methods, results such as tumor response to radiation, toxicity and survival, as well as the radiation exposure rates of healthy cells, are evaluated. It is evaluated that the exposure rate of neighboring cells is minimized in the radioembolization method with Y90[55].

2.2.3 Yttrium-90

Yttrium-90 is a radioactive isotope of yttrium, characterized by its applications in various fields, particularly in nuclear medicine. This synthetic isotope, with a half-life of approximately 64.1 hours, decays by beta emission to stable zirconium-90 (Zr-90), releasing a maximum energy of 2.28 MeV[57,58]. Yttrium-90 has garnered significant attention in the medical community due to its efficacy in radiotherapy, specifically in treating various types of cancer[59,60]. The first feature that should be taken into consideration is that Yttrium-90 undergoes beta decay, emitting high-energy beta particles (electrons). These particles have a short penetration depth in biological tissues, typically around 2.5 to 11 mm, making them effective for targeting and destroying malignant cells while sparing surrounding healthy tissues[61,62]. The half-life of Yttrium-90 is 64.1 hours, which is optimal for clinical use, providing a balance between delivering a therapeutic dose of radiation and ensuring the isotope decays relatively quickly, minimizing long-term radiation exposure[57,58].

2.2.3.1 Medical Applications of Yttrium-90

Yttrium-90 has become a cornerstone in the treatment of certain types of cancer, particularly through its use in radiopharmaceuticals for targeted therapy. As already mentioned one of the primary uses of Yttrium-90 is in treating liver cancer through a procedure known as radioembolization. This localized treatment helps to shrink tumors and alleviate symptoms, often improving survival rates and quality of life for patients with hepatocellular carcinoma or metastatic liver disease[61,63] Yttrium-90 is used in labeled monoclonal antibodies or peptides for radioimmunotherapy. The monoclonal antibody targets specific antigens on cancer cells, and the attached Yttrium-90 delivers targeted radiation, thereby minimizing damage to healthy tissues [59,60].

3
MATERIALS AND METHODS

3.1 Materials

In this study, phantoms modeled and produced Kesmezacar et al., taking into account the real structure of liver and lung, were used[6,64,65]. The main reason why the phantoms, whose detailed features will be given below, were chosen for use in this study is that both phantoms were designed to be able to inject radionuclide and model tumors. The phantom used contains only the liver and lungs and is placed fixedly in a box made of plexiglass material. The side covers of this box surrounding the phantom will represent the organs in the anatomical structure according to their distance from the liver and lungs. Yttrium-90 was used as the radionuclide, the amount and properties of which will be explained in the relevant section. Thermoluminescence dosimeters were used during radiation dose measurements. The number of dosimeters used and the dosimeter reader system will be explained in the relevant section.

3.1.1 Phantoms and Their Structures

3.1.1.1 Lung Phantom and Its Features

The phantom used in the study was modeled and produced by Kesmezacar et al. for educational and research purposes. During the modeling and production stages, care was taken to ensure that it resembles human anatomy[6]. The fact that the radionuclide can be easily transferred to the phamtom and leakage of the radionuclide is prevented by gasketed screws is one of the main reasons why it was preferred in this study. The lung model was designed with a graphic design program called Zbrush. Images showing the internal and external structure of the desing are shown in Figure 13 and Figure 14.

Figure 13 External structure of the lung

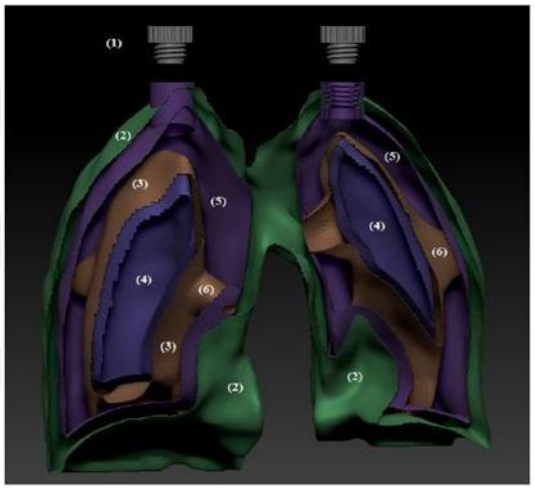

Figure 14 Internal structure of the lung

Explanations of the internal structure of the lung model shown in Figure 14 are as follows.

(1) Screw and gasket slots located at the apex of the lung.

(2) The area colored green shows the outermost part of the entire model.

(3) The section colored brown is the section that will ensure the distribution of the radionuclide parallel to the lung parenchyma surface.

(4) It is inner part of the second section colored in green. There is an air gap in this section.

(5) It is the gap between the parenchymal surface and the inner surface and has an average width of 1-2 cm. It is the part where the radionuclide to be filled from the seal slots will accumulate.

(6) It shows the support legs created to keep the section within the parenchymal surface of the lung parallel to the surface.

When the internal structure of the lung model is examined, the internal cavity volume of the right lung is 500 ml and the internal cavity volume of the left lung is 440 ml. The total volume of the phantom is 1987 ml. When viewed from the medial part, the left lung is 20 cm long and the right lung is 19 cm long. The anteroposterior width of the right lung is 13 cm while left lung is 11 cm[6].

3.1.1.2 Liver Phantom and Its Features

The most important factor in choosing the liver phantom was the internal structure of the liver model. The large and small tumor cavities in the internal structure of the liver phantom modeled and produced by Yeyin et al. and the presence of gasketed screw slots that allow the radionuclides to be used in the studies to be safely filled into these cavities increased the effectiveness of the study. The internal and external structure of the liver model is as shown in Figure 15 and Figure 16 [65].

Figure 15 External structure of the liver

Figure 16 Internal structure of the liver model

Explanations of the internal structure of the lung model shown in Figure 16 are as follows.

(1) Large tumor within the liver phantom.

(2) Small tumor within the liver phantom.

(3) Channel opening into the external lateral tumor cavity.

Additionally, Figure 17 shows the slots opening to the channels to be injected with radionuclide and their leak-proof covers.

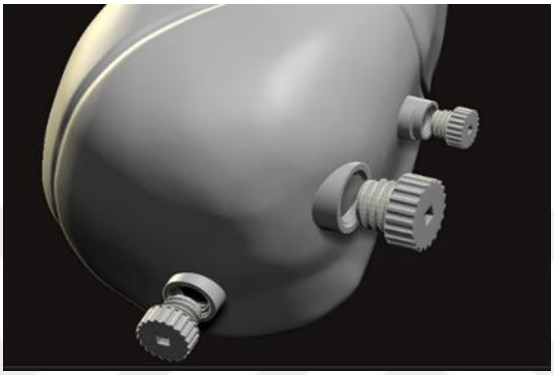

Figure 17 Phantom's radionuclide-injected sections and sealed covers.

3.1.2 Yttrium-90

During the study, Yttrium-90 radionuclide was used to model radioembolization treatment. It is known that the half life of Yttrium-90 is 2.67 days[47]. A total of 2 GBq of Yttrium-90 was injected into the liver.

3.1.3 TLDs

Thermoluminescence dosimeters were used as dosimeters in the study. A total of 24 dosimeters were placed in 12 different strategic sections on the right and left lobes of the lung. Radiation measurements were made with 18 dosimeters placed in 9 strategically determined areas on the liver. The TLDs used are as seen in Figure 18. The TLD reader used to calculate the measured dose is shown in Figure 19.

Figure 18 There are two TLDs in each of the yellow, blue and red tags.

Figure 19 TLD reader, Harshaw 4500

3.2 Methodology

During the study, the hepatopulmonary shunt model was designed by Yeyin et al. and consisted of three separate parts: lung, liver and plexiglass box. During the study, 2 GBq of Yttrium-90 radionuclide was injected into the liver. In addition to this, considering the hepatopulmonary shunt rate determined as 10%, 0.2 GBq activity, corresponding to 10% of the 2GBq activity, was applied to the lungs. Considering that the half-life of Yttrium-90 is 2.67 days, the radionuclide was left in the liver phantom for 14 days. During the study, a total of 24 TL dosimeters were

integrated into 12 different strategic parts of the lung phantom on the hepatopulmonary shunt model. By placing 2 dosimeters in each region, the aim was for the dosimeters to control each other. 18 TL dosimeters were placed in 9 different strategic regions of the liver phantom. As in the lung phantom, 2 TL dosimeters were used for each section. By measuring the total dose level to which TLDs were exposed at the end of the 14th day, the 14-day total dose level in each region where TLDs were located was determined. The dose levels to which the liver, lung and surrounding organ-tissues are exposed are shown in Table 10, Table 11 and Table 12, respectively, in the results section.

Figure 20 Hepatopulmonary shunt model and positioning of TL dosimeters on the model. T indicates; The top wall midpoint of the box. R indicates; The midpoint of the wall to the right of the box. L indicates; The midpoint of the wall to the left of the box. B indicates; The bottom wall midpoint of the box.

4
RESULTS AND DISCUSSION

4.1 Result

4.1.1 Dose Level to which the Liver is Exposed

The radiation dose level to which the liver was exposed was measured with an 18 TL dosimeter placed in 9 different regions. The measured values were converted into mathematical output with the Harshaw 4500 TLD reader and shown in Table 10. When the results are examined, it is seen that the dose levels exposed to the lower wall of the right lobe and the lower wall and rear wall of the left lobe are measured to be high. The average dose levels for these regions were measured as 2.83 Sv, 4,984 Sv, 13.725 Sv and 22.433 Sv, respectively. Considering the liver model, it was seen that the areas exposed to high dose levels were close to the back wall of the model and also in the lower part. It was evaluated that this result occurred due to the precipitation of the used resin Yttrium-90. Differences between the two dosimeters placed at each side were checked and no significant differences were observed between dose levels. Based on this, it can be interpreted that TLD measurements are reliable. Table 10 shows the minimum and maximum radiation dose levels measured in the same area.

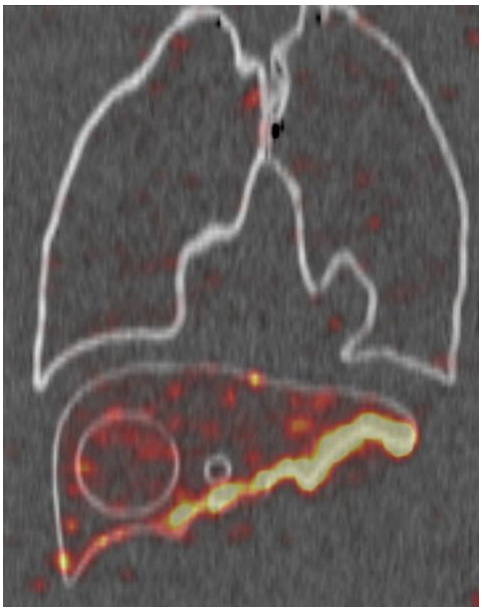

Figure 21 Visualization of radiation activities of lung and liver models with CT.

Table 10 The dose amounts measured for 9 different regions were measured with two different TL dosimeters for each region.

Location of TLDs and their distribution according to regions on the liver (Couinaud)	**Min Radiation (Sv)**	**Max Radiation (Sv)**	**Average Radiation (Sv)**
Small tumor right lobe anterior wall **(5)**	0.360	0.498	0.429
Large tumor right lobe anterior wall **(6)**	0.359	0.362	0.360
Right lobe outer lateral wall **(7)**	0.581	0.746	0.663
Anterior wall of left lobe **(3)**	0.422	0.446	0.434
Upper wall of left wall **(2)**	2.539	3.121	2.83
Upper wall of right hepatic wall **(8)**	0.721	0.847	0.784
Right hepatic lobe inferior wall **(6)**	4.524	5.714	4.984
Left hepatic lobe inferior wall **(4)**	12.902	14.549	13.725
Posterior wall of right hepatic lobe **(5)**	19.79	25.077	22.433

4.1.2 Dose Level to which the Lung is Exposed

In liver tumor treatment, the dose levels to which the lung was exposed were measured with 24 TL dosimeters placed in different regions and the values stated in Table 11 were obtained. In the examinations, the highest dose level was measured in the middle posterior wall of the left lung. The measured dose value was determined between 1.4091 Sv and 1.845 Sv. The dose values measured for each region were examined and no result was found among the results measured by the dosimeters, indicating that there was an error caused by the dosimeter.

Table 11 The dose amounts measured for 12 different regions were measured with two different TL dosimeters for each region.

Location of TLDs	Min Radiation (Sv)	Max Radiation (Sv)	Average Radiation (Sv)
Left lung apex	0.0698	0.0745	0.072
Right lung apex	0.0273	0.0383	0.0328
Left lung base	0.0641	0.0837	0.0739
Right lung base	0.0261	0.0396	0.0328
Inner side wall of left lung	0.3369	0.3463	0.3416
Inner side wall of right lung	0.6353	0.6527	0.644
Anterior wall of left lung	0.0378	0.0404	0.0391
Anterior wall of right lung	0.0406	0.0414	0.041
Middle outer side wall of left lung	0.0537	0.0584	0.0560
Middle outer side wall of right lung	0.0371	0.0403	0.0387
Middle posterior wall of left lung	1.1845	1.4091	1.296
Middle posterior wall of right lung	0.4535	0.6738	0.563

4.1.3 Dose Levels Measured Around the Liver Phantom

16 different TLDs were positioned in 8 different strategic regions in the plexiglass box in which the liver and lung phantoms were placed in a fixed manner. Considering the regions where the liver and lung phantoms were positioned in the box, each TLD placed in the plexiglass was planned to represent an organ. Table 12 shows the dose levels measured by 16 TLDs placed in 8 different sections in the plexiglass.

Table 12 Dose levels measured by TLDs on the plexiglass box surrounding the lung and liver phantoms and shows corresponding organs.

Location of TLDs	Corresponding Organ	Min Radiation (Sv)	Max Radiation (Sv)	Average Radiation (Sv)
The midpoint of the wall to the right of the box	Skin (Body)	0.089	0.218	0.153
The bottom point of the wall to the right of the box	Kidneys	0.223	0.361	0.292
The top of the wall to the right of the box	Skin (Neck)	0.013	0.018	0.015
The bottom point of the wall to the left of the box	Kidneys	0.630	0.682	0.656
The midpoint of the wall to the left of the box	Stomach	0.035	0.070	0.0525
The top of the wall to the left of the box	Skin (Neck)	0.020	0.033	0.0265
The top wall midpoint of the box	Esophagus	0.0366	0.0368	0.0367
The bottom wall midpoint of the box	Intestines	0.987	1.242	1.114

Figure 22 shows the distribution of human internal organs within the body. The analysis of the positioning of the TLDs on the plexiglass with this image is shown in Table 12.

When the results are examined, it is seen that the highest dose level is measured by the TLDs located at the upper middle point of the plexiglass box. The measurement result appears as 1.242 Sv.

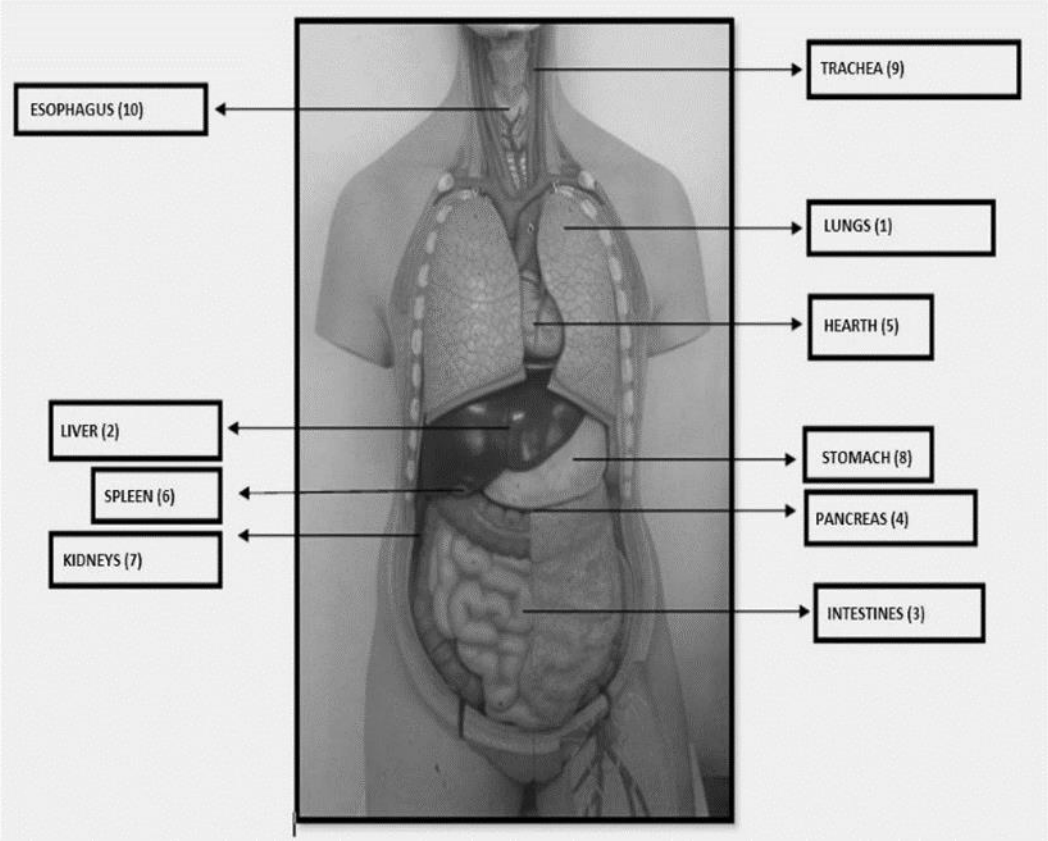

Figure 22 Internal organs of the human body.

4.2 Discussion

It has been shown in the literature that Y-90 radioembolization generally results in high doses of radiation delivered to tumor areas and that these high doses are effective in tumor control[67,68]. These high doses may be promising in terms of tumor control and shrinkage. The structure and parts of the liver are shown in Figure 10. In this image the liver is shown in 8 sections. In our study, the areas where small and large tumors were located are in segments 5 and 6. The data resulting from our measurements support that Y-90 radioembolization provides effective tumor control by delivering high localized doses to liver tumors. However, the fact that the resin Yttrium-90 we used is heavier than water and tends to precipitate caused high dose levels to be measured in the lower and back part of the liver model, not

directly in the tumor area. When the measurement results of the TL dosimeters in Table 10 and the CT images showing the activity of the liver model in Figure 21 are examined, the liver segments where the dose levels are seen to be high are segments 2, 6, 4 and 5. The locations of liver segments 4, 5 and 6, where dose levels were measured as high, confirm that the activity has bottomed out. It was evaluated that the average activity of 2.83 Sv seen in segment 2 of the liver was affected by the activity of both liver and lung. Considering the dose levels to which the lung is exposed, the fact that the highest dose level is seen in the middle lower wall of the left lung lobe, located just above the number 2 liver segment, confirms this assessment.

The dose level to which the lung was exposed was examined, and as a result of comparing all measured areas, the highest exposure level was detected in the middle posterior wall of the left lung. When the dose level exposed to both lobes was compared, it was seen that the dose level exposed to the left lobe was relatively higher than the dose level exposed to the right lobe. It was considered that the reason for the higher dose level in the left lobe of the lung was its proximity to the left lobe of the liver, where most of the 2 GBq radiation injected into the liver was emitted. The detected value was determined to be between 1.4091 and 1.1845 Sv. As a result of the literature review, although studies showing the lung's response to exposure to this specific dose are limited, it is known that similar dose exposures increase the risk of cancer and may have important health consequences. The measured value is above 1 Sv, which is accepted as the acute radiation threshold by WHO[66].

When the measurement results obtained from the TL dosimeters placed on the Plexiglas box were examined, it was seen that the highest radiation dose level was detected in the intestine section located at the bottom of the liver, with 1.242 Sv. The intestines were followed by the kidneys with 0.682 Sv. The reason why the highest dose level was seen in the intestines was evaluated as its proximity to the area where the radionuclide was injected.

5
CONCLUSION

5.1 Conclusion

In this study, which aims to determine the dose levels to which the liver, lungs and surrounding internal organs are exposed in the treatment of liver tumor by radioembolization method, the highest dose level to which the liver is exposed was measured as 25,077 Sv. The highest dose level to which the lung was exposed was 1.4091 Sv. When the dose levels to which the surrounding tissues and organs were exposed were examined, the highest dose level was measured in the intestines as 1.242 Sv.

When the measured dose levels and areas of intense activity were examined, it was observed that the Yttrium-90 resin used in the study precipitated on the lower and back walls of both the liver and lung models because it was heavier than water. This shows that the injected radionuclide is distributed heterogeneously rather than homogeneously as expected. Due to this non-homogeneous distribution, approximately 85% of the total activity is concentrated in a certain region, while 15% of the total dose is distributed in lower amounts and in different regions. This undesirable distribution shows that the high radiation levels measured during the simulation of the treatment can also affect healthy tissues and shows that the preparations made during the application of the treatment play a vital role in the healthy management of the treatment.

Despite the erroneous distribution of the radionuclide injected into the hepatopulmonary shunt model, the findings of this study may help us better understand the role of radioembolization therapy with Yttrium-90 in tumor treatment and may provide the basis for optimizing this method. Considering the advantages of the hepatopulmonary shunt model used in the study (leakage, not causing fluid resorption in tumor models, etc.) has been a good tool to reveal the effective role played by such models in determining exposure dose levels. Considering the importance of radiation protection, it has been seen that the data obtained has the potential to be evaluated and can provide insight both in terms of

reviewing the dose levels to be applied in treatments and developing the treatment method.

REFERENCES

[1] Mustafa Karabiçici, "*Inducible Pluripotent Stem Cell (iPSCs) Derived Hepatic Organoids for Modeling Liver Cancer*."

[2] Dr. Müjgan Yıldız Orman, "*Karaciğer'in Primer ve Sekonder Tümörlerinde Yttrium-90 Radyoembolizasyon Tedavisi*."

[3] D. I. Tsilimigras, P. Brodt, P. A. Clavien, R. J. Muschel, M. I. D'Angelica, I. Endo, R. W. Parks, M. Doyle, E. de Santibañes, and T. M. Pawlik, "*Liver metastases,"* *Nat. Rev. Dis. Primers*, vol. 7, no. 1, p. 27, Apr. 2021, doi: 10.1038/s41572-021-00261-6.

[4] Dr. Burak Demir, "*Karaciğer Tümörlerinde Transarteriyel Radyoembolizasyon (TARE) Tedavisi Sonrası Alınan Y-90 Görüntüleri ile Yapılan Doz Hesabı ve Tedavi Cevabının Öngörülmesindeki Rolü*."

[5] S. M. Srinivas, N. Natarajan, J. Kuroiwa, S. Gallagher, E. Nasr, S. N. Shah, F. P. DiFilippo, N. Obuchowski, B. Bazerbashi, N. Yu, and G. McLennan, "*Determination of Radiation Absorbed Dose to Primary Liver Tumors and Normal Liver Tissue Using Post-Radioembolization (90)Y PET*," *Front. Oncol.*, vol. 4, p. 255, Oct. 2014, doi: 10.3389/fonc.2014.00255.

[6] D. Viñal, A. Minaya-Bravo, I. Prieto, J. Feliu, and N. Rodriguez-Salas, "*Ytrrium-90 transarterial radioembolization in patients with gastrointestinal malignancies*," *Clin. Transl. Oncol.*, vol. 24, no. 5, pp. 796-808, May 2022, doi: 10.1007/s12094-021-02745-z.

[7] N. Yeyin, F. F. Kesmezacar, D. Tunçman, Ö. Demir, L. Uslu-Beşli, O. Günay, and M. Demir, "*Hepatopulmonary Shunt Ratio Verification Model for Transarterial Radioembolization,"* *Curr. Radiopharm.*, Jan. 2024, doi: 10.2174/0118744710284130240108053733.

[8] S. R. Mehta, V. Suhag, M. Semwal, and N. Sharma, "*Radiotherapy: Basic Concepts and Recent Advances*," *Med. J. Armed Forces India*, vol. 66, no. 2, pp. 158-162, Apr. 2010, doi: 10.1016/S0377-1237(10)80132-7.

[9] M. Donya, M. Radford, A. ElGuindy, D. Firmin, and M. H. Yacoub, "*Radiation in medicine: Origins, risks and aspirations*," *Glob. Cardiol. Sci. Pract.*, vol. 2014, no. 4, pp. 437-448, Dec. 2014, doi: 10.5339/gcsp.2014.57.

[10] F. Nüsslin, "*Wilhelm Conrad Röntgen: The scientist and his discovery*," *Phys. Med.*, vol. 79, pp. 65-68, Nov. 2020, doi: 10.1016/j.ejmp.2020.10.010.

[11] H. Yılmaz, "*RATLARDA İYONİZAN RADYASYONUN NEDEN OLDUĞU RENAL HASARA KARŞI KIRMIZI GİNSENG VE AMİFOSTİNİN KORUYUCU ETKİSİ*."

[12] G. Usta, "*RADYASYON ÇALIŞANLARINDA GÖZYAŞI FONKSİYON TESTLERİNİN VE KORNEA ENDOTEL TABAKASI ÖZELLİKLERİNİN RADYASYON MARUZİYETİYLE İLİŞKİSİNİN DEĞERLENDİRİLMESİ*."

[13] L. E. Amrani, T. Mazri, and N. Hmina, "*The Specific Absorption Rate induced in human organs due Ionizing and Non Ionizing Radiations exposure*," in *2018 6th International Conference on Wireless Networks and Mobile

Communications (WINCOM)*, Marrakesh, Morocco, 2018, pp. 1-4, doi: 10.1109/WINCOM.2018.8629631.

[14] T. Ruff, "*Health implications of ionising radiation*," 2017, doi: 10.22459/LF.09.2017.08.

[15] G. Sgouros, "*Alpha-particles for targeted therapy*," *Adv. Drug Deliv. Rev.*, vol. 60, no. 12, pp. 1402-1406, Sep. 2008, doi: 10.1016/j.addr.2008.04.007.

[16] F. Heßberger, S. Hofmann, and D. Ackermann, "*Fine structure in the α-decay of radium isotopes with mass numbers 209-212*," *Eur. Phys. J. A*, vol. 16, pp. 365-370, 2003, doi: 10.1140/epja/i2002-10111-0.

[17] A. A. H. Zarkoonsh, "*Determination of Optimal Material as TLD Device for Radiation Dosimetry Application*."

[18] U.S. Department of Energy, "*DOE Explains...Beta Decay*," [Online]. Available: https://www.energy.gov/science/doe-explainsbeta-decay. [Accessed: Jul. 7, 2024].

[19] Z. N. Demirci, "*Bremsstrahlung Foton Işinimi İçin Radyatör Parametrelerinin Belirlenmesi.*"

[20] N. Karmaker, et al., "*Fundamental characteristic and application of radiation*."

[21] B. Gültekin, *"Research and Development of ABS Filament's Capability for Gamma and Neutron Radiation Shielding*."

[22] S. Prabhu, et al., "*J. Phys.: Conf. Ser.*," vol. 1712, p. 012036, 2020.

[23] National Institutes of Health, "*Radiation Quantities and Units, Definitions, Acronyms,"*[Online].Available:https://www.ncbi.nlm.nih.gov/books/NBK230653/. [Accessed: Jul. 7, 2024].

[24] United Nations Scientific Committee on the Effects of Atomic Radiation, "*Sources and Effects of Ionizing Radiation*," UNSCEAR 2000 Report to the General Assembly.

[25] Australian Radiation Protection and Nuclear Safety Agency, "*Units of ionizing radiation measurement,"* [Online]. Available: https://www.arpansa.gov.au/understanding-radiation/what-is-radiation/radiation/measuremen. [Accessed: Jul. 7, 2024].

[26] McCollough CH, Schueler BA. Calculation of effective dose. Med Phys. 2000 May;27(5):828-37. doi: 10.1118/1.598948. PMID: 10841384.

[27] A. Tootell, K. Szczepura, and P. Hogg, "*An overview of measuring and modelling dose and risk from ionising radiation for medical exposure*," *Radiography*, vol. 20, 2014, doi: 10.1016/j.radi.2014.05.002.

[28] Division of Human Health, Medical Physics and Safety Section, "*Radiation Dosimeters.*"

[29] S. Aldelaijan, H. Mohammed, N. Tomic, L. H. Liang, F. Deblois, A. Sarfehnia, W. Abdel-Rahman, J. Seuntjens, and S. Devic, "*Radiochromic film dosimetry of HDR (192)Ir source radiation fields*," *Med. Phys.*, vol. 38, no. 11, pp. 6074-6083, Nov. 2011, doi: 10.1118/1.3651482.

[30] T. Rivera, "*Thermoluminescence in medical dosimetry,"* *Appl. Radiat. Isot.*, vol. 71 Suppl, pp. 30-34, Dec. 2012, doi: 10.1016/j.apradiso.2012.04.018.

[31] A. B. Rosenfeld, G. Biasi, M. Petasecca, M. L. F. Lerch, G. Villani, and V. Feygelman, "*Semiconductor dosimetry in modern external-beam radiation therapy*," *Phys. Med. Biol.*, vol. 65, no. 16, p. 16TR01, Aug. 2020, doi: 10.1088/1361-6560/aba163.

[32] N. Frane and A. Bitterman, "Radiation Safety and Protection," in *StatPearls [Internet]*, Treasure Island (FL): StatPearls Publishing, May 2023. [Online]. Available: https://www.ncbi.nlm.nih.gov/books/NBK230653/. [Accessed: Jul. 7, 2024].

[33] V. Tsapaki, S. Balter, C. Cousins, O. Holmberg, D. L. Miller, P. Miranda, M. Rehani, and E. Vano, "*The International Atomic Energy Agency action plan on radiation protection of patients and staff in interventional procedures: Achieving change in practice*," *Phys. Med.*, vol. 52, pp. 56-64, Aug. 2018, doi: 10.1016/j.ejmp.2018.06.634.

[34] N. Hamada and Y. Fujimichi, "*Classification of radiation effects for dose limitation purposes: history, current situation and future prospects*," *J. Radiat. Res.*, vol. 55, no. 4, pp. 629-640, Jul. 2014, doi: 10.1093/jrr/rru019.

[35] U.S. Environmental Protection Agency (EPA), "*Radiation Protection Guidance for Diagnostic and Interventional X-Ray Procedures*," Publication No. EPA-402-R-10003, Federal Guidance Report #14, 2014.

[36] U.S. Nuclear Regulatory Commission, 2020.

[37] J. Cuttler, "*Application of Low Doses of Ionizing Radiation in Medical Therapies*," *Dose-Response*, vol. 18, Jan. 2020, doi: 10.1177/1559325819895739.

[38] D. S. Gooden, "*Radium in Humans: A Review of U.S. Studies*," *Med. Phys.*, vol. 22, no. 2, pp. 2124-2125, 1995, doi: 10.1118/1.597659.

[39] E. J. Calabrese, G. Dhawan, R. Kapoor, and I. Iavicoi, "*Calabrese et al. respond to 'Radiation hormesis: Historical and current perspectives'*," *Dose-Response*, vol. 13, no. 3, pp. 1-4, 2015.

[40] E. J. Calabrese, G. Dhawan, and R. Kapoor, "*Use of X rays in the treatment of gas gangrene: A historical assessment*," *Dose-Response*, vol. 13, no. 3, pp. 1-7, 2015.

[41] Z. Chen, Z. Wu, T. A. Muluh, S. Fu, and J. Wu, "*Effect of low-dose total-body radiotherapy on immune microenvironment*," *Transl. Oncol.*, vol. 14, no. 8, p. 101118, Aug. 2021, doi: 10.1016/j.tranon.2021.101118.

[42] E. Calabrese, G. Dhawan, R. Kapoor, and W. Kozumbo, "*Radiotherapy treatment of human inflammatory diseases and conditions: Optimal dose*," *Human Exp. Toxicol.*, vol. 38, no. 8, pp. 888-898, Aug. 2019, doi: 10.1177/0960327119846925.

[43] M. Y. Orman, "*Karaciğer'in Primer ve Sekonder Tümörlerinde Yttrium-90 Radyoembolizasyon Tedavisi."*

[44] M. Hızal, "*Karaciğer Tümörlerinde Yapılan Anjiyografik Hepatik Arteriyel Tedaviler Sırasında C Kollu Bilgisayarlı Tomografi ile Tümör ve Parankim Kan Hacminin Özgün Bir Yazılım ile Değerlendirilmesi*."

[45] R. M. Juza and E. M. Pauli, "*Clinical and surgical anatomy of the liver: a review for clinicians*," *Clin. Anat.*, vol. 27, no. 5, pp. 764-769, Jul. 2014, doi: 10.1002/ca.22350.

[46] H. Abe and K. Kamimura, "*Basics, Epidemiology, Diagnosis, and Management of Liver Tumor*," *J. Clin. Med.*, vol. 12, no. 2, p. 524, Jan. 2023, doi: 10.3390/jcm12020524.

[47] S. M. Srinivas, N. Natarajan, J. Kuroiwa, S. Gallagher, E. Nasr, S. N. Shah, F. P. DiFilippo, N. Obuchowski, B. Bazerbashi, N. Yu, and G. McLennan, "*Determination of Radiation Absorbed Dose to Primary Liver Tumors and Normal Liver Tissue Using Post-Radioembolization (90)Y PET*," *Front. Oncol.*, vol. 4, p. 255, Oct. 2014, doi: 10.3389/fonc.2014.00255.

[48] L. Cicalese, "*Hepatocellular Carcinoma (HCC)*."

[49] J. Bruix and M. Sherman, "*Management of hepatocellular carcinoma: an update*," *Hepatology*, vol. 53, no. 3, pp. 1020-1022, Mar. 2011, doi: 10.1002/hep.24199.

[50] National Cancer Institute, "*Metastatic Cancer*," [Online]. Available: https://www.cancer.gov/types/metastatic-cancer. [Accessed: Jul. 7, 2024].

[51] D. I. Tsilimigras, P. Brodt, P. A. Clavien, R. J. Muschel, M. I. D'Angelica, I. Endo, R. W. Parks, M. Doyle, E. de Santibañes, and T. M. Pawlik, "*Liver metastases*," *Nat. Rev. Dis. Primers*, vol. 7, no. 1, p. 27, Apr. 2021.

[52] F. Calderon Novoa, V. Ardiles, E. de Santibañes, J. Pekolj, J. Goransky, O. Mazza, R. Sánchez Claria, and M. de Santibañes, "*Pushing the Limits of Surgical Resection in Colorectal Liver Metastasis: How Far Can We Go?*" *Cancers (Basel)*, vol. 15, no. 7, p. 2113, Apr. 2023, doi: 10.3390/cancers15072113.

[53] S. Pathak, R. Jones, J. M. Tang, C. Parmar, S. Fenwick, H. Malik, and G. Poston, "*Ablative therapies for colorectal liver metastases: a systematic review*," *Colorectal Dis.*, vol. 13, no. 9, pp. e252-e265, Sep. 2011, doi: 10.1111/j.1463-1318.2011.02695.x.Colorectal Dis. 2011 Sep;13(9):e252-65. doi: 10.1111/j.1463-1318.2011.02695.x. PMID: 21689362.

[54] H. Y. Yang, B. Jin, G. Xu, L. J. Sun, S. D. Du, and Y. L. Mao, "*Transarterial radioembolization with Yttrium-90: current status and future prospects*," *Gastroenterol. Rep. (Oxf).*, vol. 8, no. 2, pp. 164-165, Jan. 2020, doi: 10.1093/gastro/goz074.

[55] A. Saini, A. Wallace, S. Alzubaidi, M. G. Knuttinen, S. Naidu, R. Sheth, H. Albadawi, and R. Oklu, "*History and Evolution of Yttrium-90 Radioembolization for Hepatocellular Carcinoma.*"

[56] R. Salem, R. Lewandowski, C. Roberts, J. Goin, K. Thurston, M. Abouljoud, and A. Courtney, "*Use of Yttrium-90 Glass Microspheres (TheraSphere) for the Treatment of Unresectable Hepatocellular Carcinoma in Patients with Portal Vein Thrombosis*," *J. Vasc. Interv. Radiol.*, vol. 15, pp. 335-345, 2004.

[57] R. Salem and K. G. Thurston, "*Radioembolization with ^90Yttrium microspheres: a state-of-the-art brachytherapy treatment for primary and secondary liver malignancies: part 1: technical and methodologic considerations,*" *J. Vasc. Interv. Radiol.*, vol. 17, no. 8, pp. 1251-1278, 2006.

[58] D. Colcher, R. M. Sharkey, D. M. Goldenberg, and M. Juweid, "*Therapeutic applications of radiolabeled antibody fragments in cancer,*" Immunologic Res.*, vol. 27, no. 2-3, pp. 515-529, 2003.

[59] G. A. Wiseman, C. A. White, M. Stabin, W. L. Dunn, W. D. Erwin, M. Dahlbom, and T. E. Witzig, "*Biodistribution and dosimetry results from a phase III study of zevalin (yttrium-90 ibritumomab tiuxetan) for treatment of recurrent non-Hodgkin's lymphoma,*" *J. Nucl. Med.*, vol. 40, no. 12, pp. 2078-2088, 1999.

[60] M. S. Kaminski, K. R. Zasadny, I. R. Francis, A. W. Milik, C. W. Ross, S. D. Moon, and R. L. Wahl, "*Radioimmunotherapy of B-cell lymphoma with [131I] anti-B1 (anti-CD20) antibody,"* *N. Engl. J. Med.*, vol. 329, no. 7, pp. 459-465, 2000.

[61] K. T. Sato, R. J. Lewandowski, M. F. Mulcahy, B. Atassi, R. K. Ryu, V. L. Gates, and R. Salem, "*Unresectable chemorefractory liver metastases: radioembolization with 90Y microspheres—safety, efficacy, and survival,*" *Radiology*, vol. 247, no. 2, pp. 507-515, 2008.

[62] C. Breedis and G. Young, "*The anatomy of the liver under various conditions,*" *Am. J. Anat.*, vol. 68, no. 2, pp. 331-367, 2014.

[63] R. Murthy, R. Nunez, J. Szklaruk, W. Erwin, D. C. Madoff, and S. Gupta, "*Yttrium-90 microsphere therapy for hepatic malignancy: devices, indications, technical considerations, and potential complications,*" *Radiographics*, vol. 25, no. 1, pp. S41-S55, 2014.

[64] F. F. Kesmezacar, D. Tunçman, and N. Yeyin, "*3 Boyutlu Baskı Teknolojisi Kullanılarak Anatomik Akciğer Araştırma ve Eğitim Fantomu Tasarım ve Üretimi,*" *IGUSABDER*, pp. 376-386, 2023.

[65] F. F. Kesmezacar, N. Yeyin, and Ö. Demir, "*Eğitim ve Araştırma Amaçlı Üç Boyutlu (3B) Baskılı Karaciğer Fantom Tasarımı,*" *Int. J. of 3D Printing Tech. Dig. Ind.*, vol. 7, no. 2, pp. 175-183, 2023.

[66] World Health Organization, "*Ionizing radiation and health effects,*" Jul. 27, 2023. [Online]. Available: https://www.who.int/news-room/fact sheets/detail/ionizing-radiation-and-health-effects. [Accessed: Jun. 11, 2024].

[67] J. Braun, R. Boda-Heggemann, N. Ernst, A. Obertacke, and A. Zamboglou, "*Radiation dose is associated with improved local control for large, but not small, hepatocellular carcinomas,*" Radiation Oncology, vol. 18, no. 1, p. 193, 2023. [Online]. Available: https://doi.org/10.1186/s13014-023-02318-0

[68] S. L. Son, H. B. Kim, S. R. Han, K. W. Song, J. H. Kim, S. K. Pyo, and H. J. Kim, "*Optimal stereotactic body radiotherapy dosage for hepatocellular carcinoma: a multicenter study,*" *Radiation Oncology*, vol. 16, no. 1, Article 176, Sep. 2021, doi: 10.1186/s13014-021-01778-6.

PUBLICATIONS FROM THE THESIS

Conference Papers

1. Determining the Radiation Dose Level to Which the Lung is Exposed in Liver Tumor Treatment – INCOHIS 2024

2. Determining the Radiation Dose Level To Which The Liver is Expoed in Liver Tumor Treatment – ICSuSaT 2024